Analyst

Accepted Manuscript

This article can be cited before page numbers have been issued, to do this please use: M. Gomez-Mingot, V. Montiel, C. E. Banks and J. Iniesta, *Analyst*, 2013, DOI: 10.1039/C3AN02137H.

ROYAL SOCIETY OF CHEMISTRY

www.rsc.org/analyst

View Article Online
DOI: 10.1039/C3AN02137H

Screen-printed graphite macroelectrodes for the direct electron transfer of cytochrome c: A deeper study of the effect of pH on the conformational states, immobilization and peroxidase activity

Maria Gómez-Mingot[a,#], Vicente Montiel[a], Craig E. Banks[b,*] and Jesús Iniesta[a,*]

[a]*Physical Chemistry Department and Institute of Electrochemistry, University of Alicante, 03690 San Vicente del Raspeig, Alicante, Spain*

[b]*Faculty of Science and Engineering, School of Science and the Environment, Division of Chemistry and Environmental Science, Manchester Metropolitan University, Chester Street, Manchester M1 5GD, Lancs, United Kingdom*

Submission to: Analyst

***Corresponding authors:**

Jesús Iniesta : E-mail: *jesus.iniesta@ua.es*; Tel: +34 965909850; Fax: +34 965903536

Craig Banks : E-mail: *c.banks@mmu.ac.uk*; Tel: +44 (0) 1612471196;

Fax: +44 (0) 1612476831

[#]**Present address**:

Nano-Electrochemistry Group, Université Paris Diderot, Sorbonne Paris Cité, ITODYS, UMR 7086 CNRS, 15 rue Jean-Antoine de Baïf, 75205 Paris Cedex 13, France.

View Article Online
DOI: 10.1039/C3AN02137H

Abstract

The direct electron transfer of cytochrome c has been studied at screen-printed graphite macroelectrodes without recourse to mediators or the need of any electrode pre-treatments as is commonly employed within the literature. A wide range of pH values from 2.0 to 11.0 have been explored upon the electrochemical response of cytochrome c and different voltammetric signatures have been observed. The direct electron transfer of the alkaline transition of cytochrome c was found impeded within alkaline media leading to either an irreversible redox process or even no voltammetric responses. In acidic aqueous media the electrochemical process is observed to undergo a mixed diffusion and adsorption controlled process rather than a purely difusional process of the native conformation as observed at pH 7.0. Interestingly, at pH 3.5 a new conformational state is revealed in cooperation with the native conformation.

The immobilization of the protein was satisfactorily obtained with a simple method by cycling the protein at specific solution pH values allowing amperometric responses to be obtained and gives rise to useful *pseudo*-peroxidase activity for sensing H_2O_2. Apparent Michaelis Menten constant values (K_m) were calculated via the Lineweaver-Burk method with deduced values of 25 ± 4, 98 ± 12 and 230 ± 30 mM, respectively for pH values of 2.0, 3.0 and 7.0. Such work is important for those utilising cytochrome c in bio-electrochemical and related applications.

Keywords: Cytochrome c; Screen-printed Electrodes; Direct Electron Transfer; Conformational States; Peroxidase Activity.

View Article Online
DOI: 10.1039/C3AN02137H

1. Introduction.

Structural changes and dynamics of intermolecular electron transfer (ET) in native cells are responsible for addressing cell membrane processes such as ion pump regulation, electric field-related treatments, ion-transport channel functioning across membranes and protein-protein interactions [1, 2]. Thus, characterization studies of proteins structural changes and their immobilization upon surfaces are vital as a means of constructing a biomimetic system able to reproduce biological mechanisms.

Cytochrome c (cyt-c) is a membrane protein responsible for the ET in the transport chain and it may exist in solution in five reversible, pH-dependent conformational states with *pKa*'s values of 0.42, 2.50, 9.35, and 12.76, denoted as states: I, II, III, IV, and V, respectively [3, 4]. The iron in the native *heme* of the protein is complexed within the porphyrin axially to a methionine (*Met80*) and a histidine (*His18*), while it is covalently attached via thioether bonds to the polypeptide backbone throughout two cysteine residues (*Cys14* and *Cys17*). Two factors make the reduction potential of the native (N) state of cyt-c (state III, -~ unusually positive values of + 0.2 V to + 0.38 V). The first is the stabilization effect of the Fe(II) state due to the π-electron accepting character of the thioether sulphur atom of *Met80* and the second is the inaccessibility to the *heme* which is buried within a hydrophobic pocket, which also favours the ferrous state beyond the ferric [5].

Non-native states of cyt-c have been studied in depth as they have a role, not fully understood, in apoptosis and cellular oxidative stress processes beyond the ET function [6, 7]. The effects on the protein stability and structure and furthermore, the influence in the *heme* coordination due to changes of pH, anionic strength and nature of the anions have been widely and extensively studied [8, 9]. In this respect, the alkaline isomerisation is known as the transition of cyt-c from neutral pH (state III) to alkaline pH (state IV) and results from the disruption of the *Met80*-Fe coordination bond and the introduction of a residue of lysine (*Lys72*) The other main covalent transition occurs at acidic pH values with the formation of the low-pH conformer (state II, *pKa* ~ 2.5) in which both axial ligands are protonated and detached from the iron, thus conforming a high spin configuration, in which axial positions are occupied by water molecules. Moreover, it has been reported that an intermediate state is formed during the process of total unfolding of the protein by the *Met80*-Fe disruption (state II). This stable state is caused by a non-covalent modification and is called the

View Article Online
DOI: 10.1039/C3AN02137H

molten globule state (MG) which has a *pKa* ~ 3.0 [10]. As explained, there are plenty of stable conformations of the protein depending of the pH value, and it is thought that the relationship of the differences between kinetic intermediates and the equilibrium of MG state could probably be the key of the protein unfolding and refolding [11- 13].

Interfacial interactions of ET between proteins and electrochemical platforms are widely studied with the aim of providing an insight into *in vivo* behaviour which can be exploited in bio-electrocatalytic systems [14, 15]. Functionalities residing at the carbon electrode surfaces, usually upon edge plane like - sites/defects ensure favourable electrostatic interactions with proteins. Studies on cyt-c immobilization on a surface of a basal plane graphite electrode in a room temperature ionic liquid [16], on silicon dioxide nanoparticles-modified electrodes [17], and on clay colloidal-membranes [18] obtained clear direct ET. Recently, we have demonstrated that screen-printed graphite electrodes (SPGEs) provide direct ET for cyt-c in aqueous solutions due to the electrostatic interaction between the positively charged *Lys* amino groups on cyt-c and the negatively charged carboxylated groups on the surface of the electrode [19]. The negative charge density of the surface depends on the solution pH, and hence the pH dependence of the ET rate is attributed to changes in the rearrangement reaction rate of cyt-c on the electrode surface. However, to the best of our knowledge the pH effect of solutions on cyt-c conformation and hence their ET characterization of different conformational states has not been yet examined on graphitic surfaces in SPGE platforms.

In this work, we employ electrochemical techniques to study the pH-dependent dynamics of the direct charge-transfer processes of cyt-c using SPGEs in a very wide range of pH values, from 2.0 to 11.0. Immobilization of cyt-c is induced by electrochemical cycling at different pH solutions and an average coverage of protein is determined with different solution pH values. Furthermore, in order to investigate the peroxidase activity of the adsorbed redox protein towards H_2O_2, the addition of increasing concentrations of this oxidizing agent resulted in the calculation of the apparent Michaelis Menten kinetic constant.

View Article Online
DOI: 10.1039/C3AN02137H

2. Materials and methods.

Materials. All chemicals used were of analytical grade and were used as received without any further purification. All solutions were prepared with deionised water of resistivity not less than 18.2 MΩ cm (Millipore, Merck, Germany). Cyt-c from horse skeletal muscle (Sigma ≥ 95 %) was used as received. The supporting electrolyte for the solutions of cyt-c was 0.1 M NaH_2PO_4 (PBS, Sigma) which gave a pH of 4.33, this solution was acidified with the addition of *o*-H_3PO_4 (85 wt. %, Sigma) to obtain solutions in the pH range of 2.0 up to 4.0 and basified with the addition of NaOH (Sigma) to obtained solutions with pH values greater up to 11.0. H_2O_2 solutions of 200 mM were prepared freshly in the convenient PBS pH value solution from dilution of H_2O_2 (50 wt. %, Sigma).

2.1. Cyclic voltammetry. Voltammetric measurements were carried out using a μ-Autolab III (Eco Chemie, The Netherlands) potentiostat/galvanostat and controlled by Autolab GPES software version 4.9 for Windows XP. All measurements were conducted using a three-electrode configuration where the working (3.1 mm diameter) and counter electrode consist of carbon with a silver/silver chloride reference electrode (pseudoAg/AgCl). The carbon-based screen printed electrodes were fabricated in-house with appropriate stencil designs using a microDEK 1760RS screen-printing machine (DEK, Weymouth, UK). First, a carbon-graphite ink formulation (Product Code: C2000802P2; Gwent Electronic Materials Ltd, UK) was screen-printed onto a polyester (Autostat, 250 micron thickness) flexible film. This layer was cured in a fan oven at 60 degrees for 30 minutes. Next a silver/silver chloride reference electrode was included by screen printing Ag/AgCl paste (Product Code: C2040308D2; Gwent Electronic Materials Ltd, UK) onto the polyester substrates. Finally, a dielectric paste (Product Code: D2070423D5; Gwent Electronic Materials Ltd, UK) was then printed onto the polyester substrate to cover the connections. After curing at 60 degrees for 30 minutes the screen-printed electrodes are ready to be used. Studies involving scan rate were performed with a solution of 0.08 mM of cyt-c in different pH values. The experimental set-up was very simple as these studies were performed in a drop covering the SPGE surface. For the comparison, formal potentials of the ET of cyt-c (E^0, expressed in mV) subjected to pH variations were referred to a Standard Reference Electrode Ag/AgCl/KCl (3.5 M). Experiments were carried out at room temperature.

View Article Online
DOI: 10.1039/C3AN02137H

2.2. Adsorption of cyt-c. A forced adsorption procedure of cyt-c on the SPGEs was electrochemically performed cycling between + 0.2 and - 0.2 V (*vs.* p*seudo*Ag/AgCl) at 100 mVs^{-1} for 100 cycles the SPGE in different PBS buffer solutions containing a protein solution concentration of 0.162 mM at room temperature and at the desired pH value. After adsorption, the SPGE was gently rinsed with Millipore water and rapidly covered with buffer PBS solution to further study the peroxidase activity.

2.3. Cyt-c peroxidase activity study. After cyt-c adsorption procedure at pH 2.0, 3.0, 4.0 and 7.0 the electrode was immersed into a PBS solution (2 mL volume cell) and waited for stabilisation of the baseline. Chronoamperometry was performed at a cathodic potential of - 0.5 V (*vs. pseudo*Ag/AgCl) under mass control conditions using a magnetic bar at constant stirring. Baseline corrections regarding the electrochemical reduction of H_2O_2 in the absence of cyt-c adsorbed onto the SPGE platform were performed for all experiments.

3. Results and discussion.

3.1. Influence of solution pH value on the electrochemistry of cyt-c/SPGE

The pH-dependent voltammetric signatures of 0.08 mM cyt-c at SPGEs were first explored over a wide pH range from 2.0 to 11.0, as depicted in Fig. 1, where Fig. 1A shows the response for pH values between 2.0 and 3.0, Fig. 1B between 3.5 and 5.0, Fig. 1C between 6.0 and 8.0 and, finally, Fig. 1D between 9.0 and 11.0.

Our previous work demonstrated that well-defined and quantifiable voltammetric responses are readily observed at physiological pH using screen-printed electrodes [19]. Any variation of the solution pH would induce conformational changes at the protein and would resonate the active site since the redox centre of cyt-c is embedded within a rigid 34 Å diameter shell with nine positive charges at pH 7.0 with a considerable dipole moment [20-23]. At pH 7.0 the dominant state of cyt-c is III (*His18* and *Met80* in axial positions of the *heme*) [24, 25], whereas at pH close to *pKa* 9.5 a conformational transition occurs between states III and IV which involves the substitution of *Met80* from the *heme*, presumably by *Lys79* [26]. The progressive loss of voltammetric ET at alkaline pH values (Fig. 1C) could be correlated to the de-

View Article Online
DOI: 10.1039/C3AN02137H

coordination of the axial *His18* and *Met80* ligands in the *heme* pocket. The conversion of cyt-c due to variation of pH from extreme values (Fig. 1A) reflects a remarkable effect on the ET kinetics and activity of the protein.

Cyclic voltammograms (CVs) presented in Fig. 1 are analysed in terms of the peak potential separation (ΔEp), formal potential ($E^{0'}$) and ET rate constant (k_s) with variation of pH (Fig. 2). As a summary, Fig. 2 shows the dependence of these parameters upon pH where the ΔEp values remain almost unchanged as it ranges from 30 mV (at 50 mVs^{-1}) at pH 2.0 to 75 mV at pH 7.0 -Fig. 2A-, whereas the $E^{0'}$ ranges from 235 mV (*vs.* standard Ag/AgCl/KCl (3.5 M)) at pH 2.0 to 174 mV (*vs.* standard Ag/AgCl/KCl (3.5 M)) at pH 7.0 -Fig. 2B. In alkaline solutions above pH 8.0, the shape of the peak broadens and the ΔEp is enlarged (Fig. 2A) and barely non-defined redox peaks are obtained (Fig. 1D). The direct ET rate constant (k_s) was calculated according to the method described by Laviron [27] for mixed diffusion and adsorption processes and under experimental conditions with ΔEp smaller than 200 mV and assuming that the number of electrons in the process is $n = 1$ and the charge-transfer coefficient α is 0.5 for 50 mVs^{-1}. Fig. 2B shows that the k_s value at pH 7.0 was 0.7 s^{-1}, while a decrease in k_s values is clearly observed at high pH values as denoted by a more irreversible ET process, 0.5 s^{-1} at pH 8.0. On the contrary, k_s values increase at lower pH values, leading for example to values of 2.4 s^{-1} and 1.1 s^{-1} at pH 2.0 and 3.5, respectively. As stated before, Fig. 2B correlates very well the variation of the ΔEp with ET rate k_s along pH. Furthermore, Fig. 2C shows how the *Ipc* / *Ipa* ratio varies with pH with a tendency towards 1.0 at pH values range from pH value 2.0 and 7.0, whereas it shows a minimum value of 0.5 at pH 3.5. Similarly, the effect of scan rate (υ) was explored over the range from 1 to 1000 mVs^{-1} showing two clear tendencies to linearity of plots regarding anodic and cathodic peak currents (*Ipa* and *Ipc*, respectively, results not shown). In the pH range between pH 2.0 and 3.5 plots of *Ipa* and *Ipc* plots against scan rate are found to be linear ($R^2 = 0.995$) denoting a predominance of adsorption-controlled process while in the pH range between pH 4.0 to 8.0 shows a linearity towards the square-root of the scan rate which is indicative of a purely diffusion-controlled process.

At extreme acidic conditions (pH 2.0), the electrochemical response of the protein shows a clear oxidation-reduction profile. Parameters obtained from the voltammetric signatures such as ΔEp and $E^{0'}$ were similar for pH values of 2.0 and 3.0. This indicates that our experimental conditions of buffer solution concentration

View Article Online
DOI: 10.1039/C3AN02137H

(0.1 M PBS) kept substantially almost unaltered the *heme* surrounding conformation and therefore the protein is not denaturalised at pH 2.0 [28, 29]. As shown above, with the increase of the solution pH from 2.0 to 8.0, $E^{0'}$ shifted very slightly to lower values giving a variation of 65 mV. Moreover, it is remarkable that the peak current ratio (*Ipc* / *Ipa)* -extracted from Fig. 1- showed a minimum value of 0.5 at pH 3.5 which would be in agreement with the plausible explanation that two species in equilibrium are being oxidised. Thus, considering that carboxylic groups on the electrode surface with *pKa* values near to 4.5, acidic pH values up to 5.0 provided a neutral protonated surface. This protonated surface interacts with positively charged amino residue groups in the protein, whereas at pH values higher than 5.0 and when the protein isoelectric point - *pI* 10.5- is reached the carboxylated groups on the surface start to compensate the $-NH_3^+$ groups and the repulsive charges between negatively charged surface and global negative charge of the protein makes the interfacial ET processes unviable.

The presence of a single species adsorbed on the electrode is evidenced as being in the native forms (N), which are oxidised and reduced on the electrode surface, another species is observed when the pH is decreased to a value near 3.5. In that respect and close to these pH values -between 3.0 and 4.0- two cathodic and anodic peaks are revealed at low scan rates, whilst at moderately higher scan rates a small shoulder can be discerned around + 0.1 V. Fig. 3 shows the simultaneous and direct ET responses for N and another acidic-dependent species with a different conformational state for different pH values, 2.5 (Fig. 3A), 3.0 (Fig. 3B), 3.5 (Fig. 3C), and 4.0 (Fig. 3D) at low scan rates (1 mVs^{-1}). Similarly, for the oxidation process I-O, the peak potential remains almost constant at pH values of 2.5 and 3.0 with *Ep* close to 50 mV whereas at pH 3.5 and 4.0 the *Ep* decreased to a value of 28 mV. Nevertheless, ΔEp resulted to be close to the theoretical *ca.* 59 mV for one electron process. The presence of a new slightly-defined reduction peak (II-R) is revealed at pH 3.5 and becomes clearer at pH 4.0 at a peak potential of about - 144 mV and - 154 mV, respectively. At the same time, at these pH values, the most striking characteristic of this study was the second oxidation peak (II-O) which appeared at - 90 mV, and most remarkably the ΔEp for both processes I and II resulted to be approximately 54 mV at pH 3.5. However, at pH 4.0, ΔEp could be estimated to be *ca.* 67 mV for the process I and *ca.* 62 mV for the process II. Moreover, under deoxygenated conditions, the electrochemical behaviour of cyt-c at pH 2.5, 3.0, 3.5

View Article Online
DOI: 10.1039/C3AN02137H

and 4.0 gave rise to the same CV trace to that described in Fig. 3 discarding that these two peaks were related to the electrochemical reduction of oxygen.

As slightly shown in Fig. 1B and further observed when applying a slow scan rate (Fig. 3), a pH-dependent acidic protein conformation which is in equilibrium with cyt-c N state is revealed and hypothesized as the MG state. MG state has a compact secondary structure and a largely disordered tertiary structure which lacks well-packed side chains but retains the hydrophobic core as in the N state [10, 12]. The most remarkable fact was the observation of a "second" anodic peak (II-O) at a peak potential of -0.1 V (Fig. 3C).

3.2. Electrochemical Properties of cyt-c Immobilized on SPGE.

Structure conformation of cyt-c is also intimately related to immobilization of cyt-c onto the SPGE platform. At acidic pH the peak current (*Ip*) showed a linear response as a function of scan rate, denoting an adsorption-controlled process. Conformational state II, where *Met80* decordinates and is presumably replaced by a molecule of H_2O, is becoming more significant and dominant at lower pH. Consequently, the *heme* pocket is more exposed to the solvent providing a slightly higher hydrophobic character to the protein and probably favoring protein-protein interactions that make possible the formation of multi-layers on the electrode surface.

We next turn to exploring the immobilization of cyt-c at different pH values by cyclic voltammetry and its electrochemical response, as depicted in Fig. 4. Figs. 4A and 4B show an increased electrochemical profile after the immobilization process (curve b) compared to the third cycle of CV response when the protein is in solution (curve a), indicating that at these pH values -2.0 and 3.0-, the protein is adsorbed and remains almost unaltered in terms of its conformation at the electrode surface.

Furthermore, under the same experimental conditions as those applied in Fig. 4A and 4B, the adsorbed protein at pH 4.0 (Fig. 4C) shows that after the immobilization process (curve b) the CV response is lower than the observed in the third scan before immobilization (curve a). Also note that the redox peaks related principally to II-O and in a lesser manner to II-R clearly observed at this pH (curve a) are discarded in the voltammetric signature of adsorbed cyt-c, suggesting that this conformation is less probable than the native one. Unfortunately, there was no evidence for the electrochemical response of the adsorbed cyt-c after cycling at pH 7.0 due to probable a less favourable interaction with the electrode surface (Fig. 4D).

View Article Online
DOI: 10.1039/C3AN02137H

The surface coverage (Γ) of the protein can be estimated according to the following Laviron equation (eq. 1):

$$Ip = n^2 F^2 A \upsilon \Gamma / 4 R T = n F Q \upsilon / 4 R T \quad (1)$$

where Γ (molcm^{-2}) is the average amount of adsorbed cyt-c on electrode surface, A is the electrode area (cm^2), n is the number of electron transferred, Q is the charge involved in the reaction and F is the Faraday's constant. Using a surface coverage calculation method [30], at a scan rate of 50 mV s^{-1}, a coverage of cyt-c gave rise to values of 4.44 x 10^{-11} mol cm^{-2}, 3.39 x 10^{-11} mol cm^{-2} and 4.31 x 10^{-12} mol cm^{-2} at pH 2.0, 3.0 and 4.0, respectively. Coverage values denote multilayers of adsorbed cyt-c onto the SPGE platform, when considering that for a theoretical monolayer of cyt-c when using a SAM-modified electrode the coverage should be 1.40 x 10^{-12} molcm^{-2} [31, 32], indicating that our measured surface coverage of cyt c is lower as the pH value increase. These results are in agreement with the fact that at low pH values the ET process is highly controlled by adsorption. In contrast, no redox peaks could be observed for the adsorption experiments carried out at pH 7.0 (as shown in Fig. 4D) meaning that the N conformation present at this physiological pH is not prone to adsorb largely on the surface of the electrode. Nevertheless, the presence of adsorbed protein was proved by the observation of catalytic activity towards the addition of H_2O_2 (Fig. 6).

3.3. Peroxidase Activity of cyt-c Immobilized on SPGE.

The structural similarities of cyt-c with the family of peroxidases, the enzyme that makes the catalysis of H_2O_2, provide cyt-c with an intrinsic activity to convert H_2O_2 to H_2O, as described in the following equations (eqs. 2 and 3):

$$\text{cyt-c\_Fe (III)} + e^- \rightarrow \text{cyt-c\_Fe(II)} \quad (2)$$

$$2\ \text{cyt-c\_Fe (II)} + 2\ H^+ + H_2O_2 \rightarrow 2\ \text{cyt-c\_Fe(III)} + 2\ H_2O \quad (3)$$

The response of cyt-c immobilized on the SPGE towards the effect of increasing amounts of H_2O_2 was performed by cyclic voltammetry in order to study the oxidative modification induced. Although the literature reports on the possible intervention of residual metals and enzymes to catalyze a range of side-reactions and produce non-specific oxidative damage via radical production, here the protein immobilization

View Article Online
DOI: 10.1039/C3AN02137H

procedure prevented metals or impurities such as protein oligomers to be present in the experiments [33]. Due to this, it is surmised that these assays evidence the effect of the oxidative modification of cyt-c due to the interaction with the Fe in the *heme* pocket and the H_2O_2 following catalysis of Fenton reaction. The *pseudo*Ag/AgCl reference electrode of the SPGE was found to be stable over the timescale of the electrochemical experiments. The effect on the reference electrode stability due to the oxidizing conditions was discarded since a very well-defined reversible ET of ferrocyanide / ferrocyanide redox couple remained unchangeable to the addition of H_2O_2 for the same H_2O_2 concentrations tested. However, from a biochemical point of view, the oxidative modification of cyt-c by H_2O_2 has been studied extensively. For example, Kang and co-workers have shown the cyt-c oligomerization caused by the protein damage via carbonyl derivatives generation and dityrosine bonds formation in the presence of H_2O_2 [33]. The oxidative damage of H_2O_2-sensitive amino acids (*Met*, *His* and *Tyrosine*) is caused by free radicals generated by a mixture of a Fenton reaction of the free iron released from the oxidative-damaged protein and its peroxidase activity in the presence of H_2O_2 [33, 34]. The oxidative damage to proteins has been widely reported to be produced by the generation of hydroxyl radical and therefore prompting a broad number of covalent modifications at proteins [35- 41].

Fig. 5A shows the steady-state current response to five successive additions of 10 μL, 0.2 M of H_2O_2 into 2 mL of 0.1 M PBS pH 2.0 subjected to continuous stirring. The H_2O_2 concentration in the bulk solution changes about 1 mM for each injection. The catalytic *Ipc* was measured at a potential of - 0.5 V (*vs. pseudo*Ag/AgCl) and it was found to increase steeply up to a "plateau" after 10 s. In Fig. 5B, the reciprocal of the catalytic *Ipc* was plotted *vs.* the reciprocal of the concentration of the substrate, in order to calculate the enzyme-substrate kinetics by using the Lineweaver-Burk plot [40, 42], as the inverse of the intercept of this plot, 14.8 μA, corresponded to the i_{max}, and from the slope the Michaelis Menten constant (K_m), 25 ± 4 mM, can be obtained for pH 2.0. Similarly, the peroxidase activity for cyt-c adsorbed at the SPGE was compared at other pH values, 3.0 and 7.0, as it is depicted in Fig. 6, curves b and c, respectively, with the same successive stepwise injections of H_2O_2 to PBS solutions. K_m values were calculated by using the Lineweaver-Burk method and resulted to be 98 ± 12 mM and 230 ± 30 mM, respectively, denoting a lower catalytic response or affinity of cyt-c towards the oxidation of H_2O_2 probably due either to the more folded conformational state of the

View Article Online
DOI: 10.1039/C3AN02137H

protein or low protein immobilised on the SPGE surface as physiological pH is reached.

Kinetics of the peroxidase activity of cyt-c adsorbed on the surface was satisfactorily studied under different pH values. Similar responses were obtained by Scheller and co-workers when they applied chronoamperometry at 0 V to their cyt-c immobilized by polishing a colloidal gold modified carbon paste electrodes on a plane glass surface with a drop of 4% cyt-c solution [43]. Wang and Waldeck [40] found similar K_m (7.9 mM) for pH 3.0 and 144 mM for pH 7.0 when cyt-c was adsorbed at carboxylic acid-terminated and hydroxyl-terminated SAMs on gold electrodes. At pH 2.0 the SPGE/cyt-c electrode exhibits a higher affinity to H_2O_2 as the protein is presumably is partially unfolded and then the *heme* pocket more exposed.

View Article Online
DOI: 10.1039/C3AN02137H

4. Conclusions.

SPGE have been shown to be explored as novel platforms with unique properties due to the oxygenated species that allow the deeper study of biological aspects of cyt-c regarding structure and function without the need of electrode surface modification as is commonly undertaken in the literature and consequently presents an easy and rapid experimental design. The signal-to-noise ratio presented in the CVs indicates clearly the utility of these electrodes for this purpose. We have examined the effect of pH on the electrochemical response of ET process of cyt-c even at very extreme acidic and alkaline conditions. Furthermore, and accordingly to the literature, it can be concluded that the reversible behaviour observed for cyt-c at pH 2.0 is caused by a high buffer concentration, while the impeded electron transfer that occurs at pH values higher than 8.0 can be due to electrostatic impediments. It has also been shown the striking co-existence of two conformations of cyt-c at pH values between 3.5- 4.0 as means of a shoulder at moderate scan rates and a clear apparition of a "second pair of redox peaks" at low scan rates at slightly more negative potentials. Peroxidase activity of the immobilized cyt-c/SPGE was satisfactorily studied for the response to H_2O_2 under different pH conditions exhibiting a higher response at pH 2.0 due to a considerable exposition of the *heme* pocket.

Our electrochemical approach for the characterization of the electron transfer of cyt-c shows relevant applications in terms of studying the effects that the oxidative stress agents can produce on electrochemical responses of proteins. For example, oxidation or nitration of cytochrome can notably alter its function and structure with consequences in electron transfer impediments, immobilization effectiveness and biosensing. The present findings will help understand the fundamentals of interfacial redox processes, and may contribute to improve the performance of biosensors, bioelectronics, and biofuel cells.

Acknowledgements

Authors would like to thank Prof. Aldaz for his fruitful contribution to the discussion of these results. Financial support from The Ministry of Science and Technology (project CTQ2010-18570) is gratefully acknowledged.

View Article Online
DOI: 10.1039/C3AN02137H

Figure 1. Cyclic voltammetric profiles of 0.08 mM cyt-c/SPGE in 0.1 M PBS at different pH values: (A) 2.0 and 3.0, (B) 3.5, 4.0 and 5.0, (C) 6.0, 7.0 and 8.0 and (D) 9.0, 10 and 11.0. Data were obtained from the CVs at a 50 mVs^{-1}. Dotted line is related to the PBS background response.

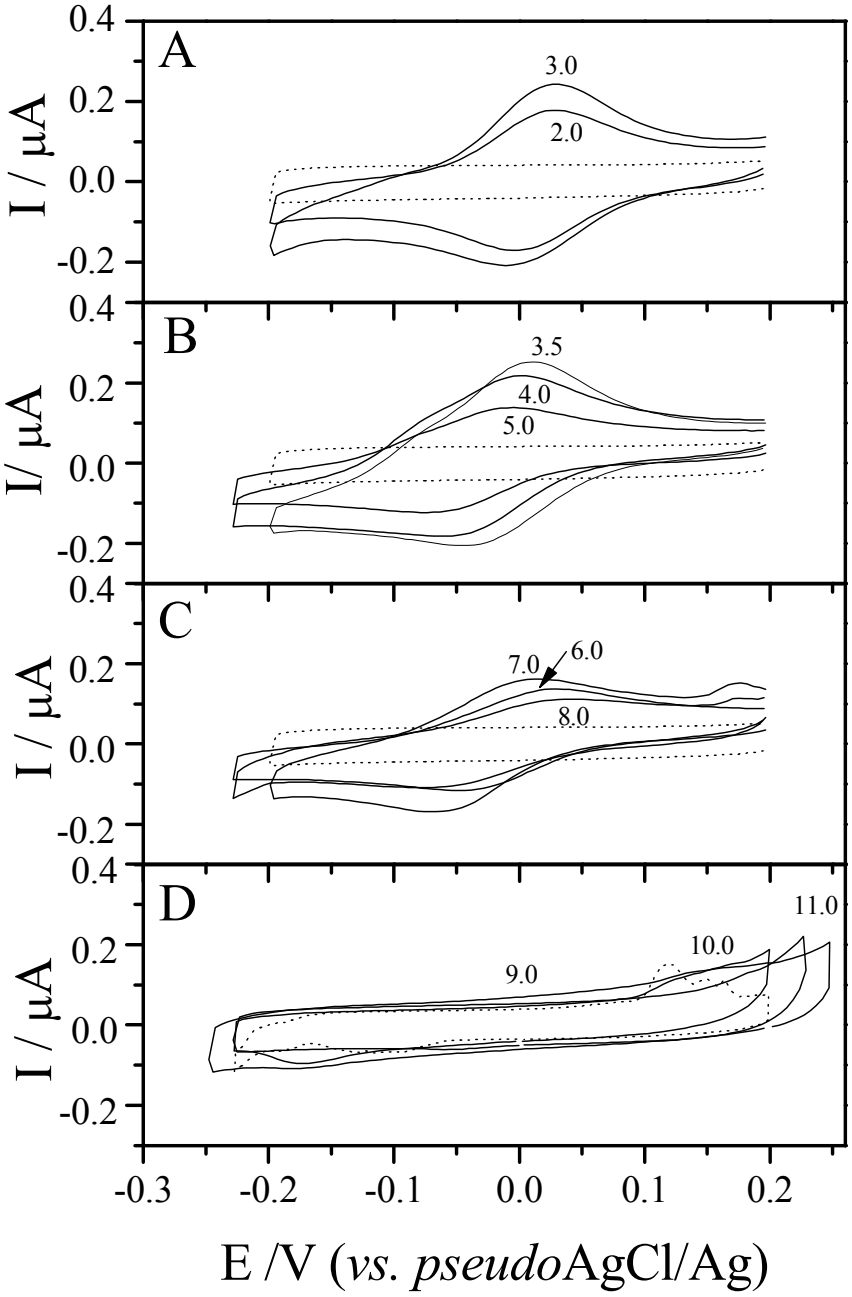

View Article Online
DOI: 10.1039/C3AN02137H

Figure 2. Dependence of current intensity peak separation (*ΔEp*/mV, open triangles) and formal potential ($E^{0'}$/ mV, dark squares) over pH (A), the ET constant variation (k_s/ s^{-1}, dark circles) *vs*. pH (B) and *Ipc / Ipa* ratio *vs*. pH (C). Data obtained for 50 mVs^{-1}.

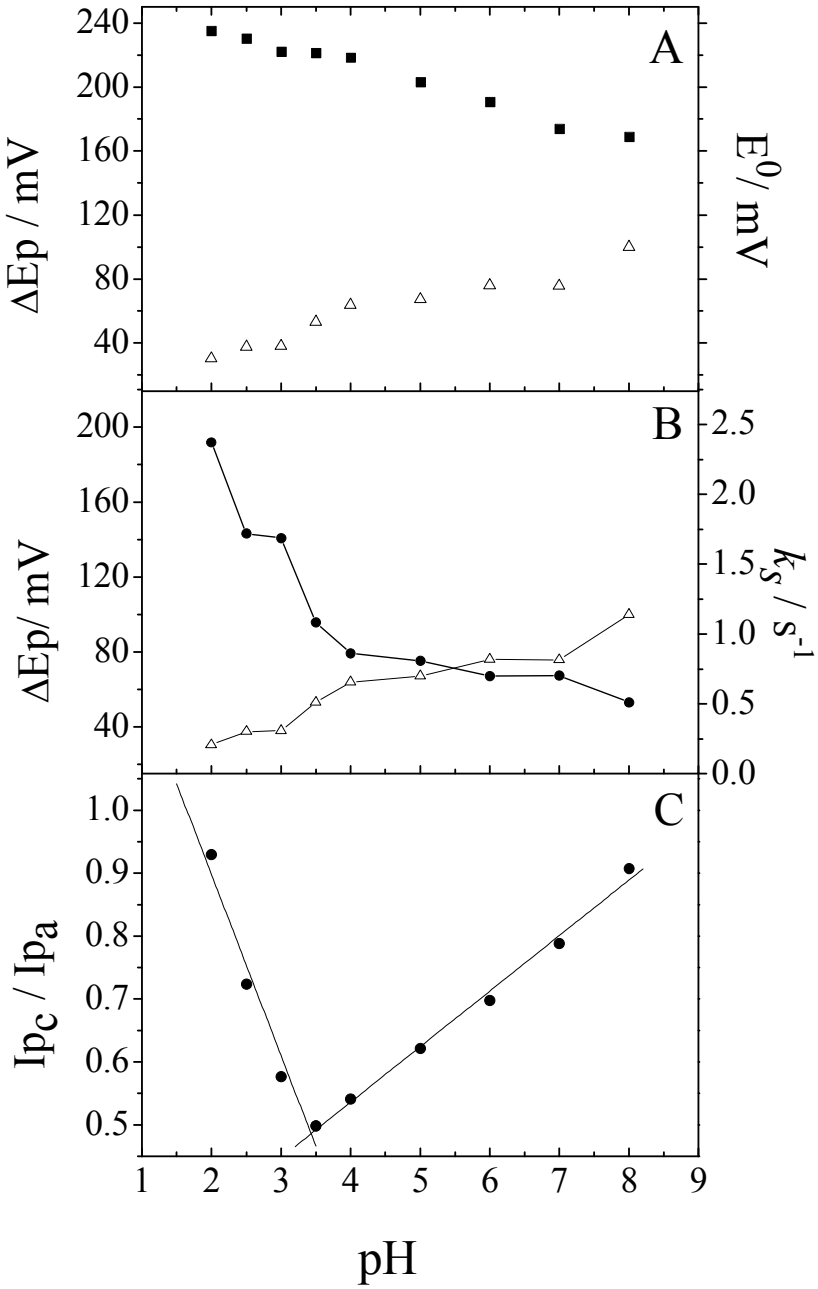

View Article Online
DOI: 10.1039/C3AN02137H

Figure 3. Cyclic voltammetric profiles of 0.08 mM cyt-c/SPGE in 0.1M PBS at different pH values: 2.5 (A), 3.0 (B), 3.5 (C) and 4.0 (D) recorded at 1 mVs^{-1}. Dotted line is related to the PBS background response.

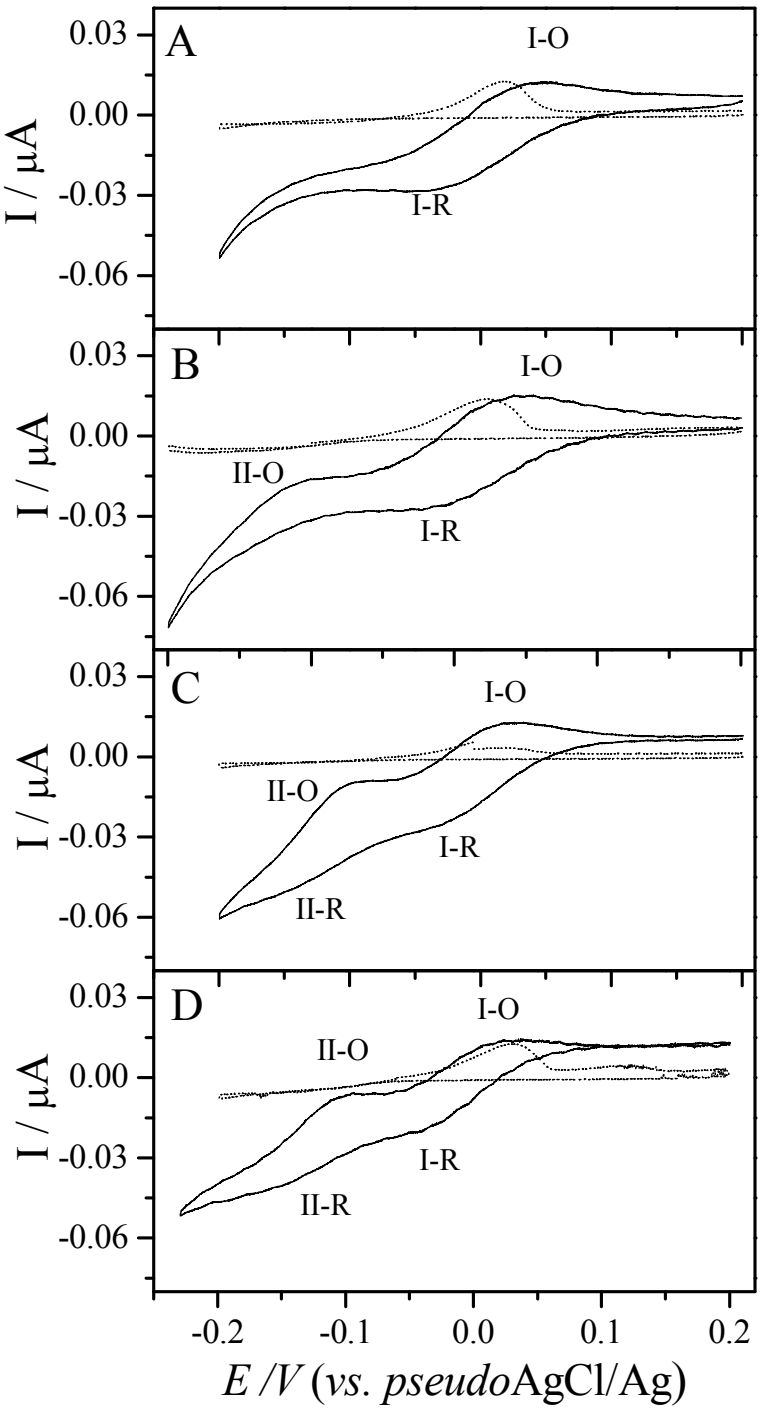

View Article Online
DOI: 10.1039/C3AN02137H

Figure 4. Cyclic voltammetric profiles of 0.162 mM cyt-c/SPGE in 0.1 M PBS before (trace a) and after the immobilization procedure at 50 mVs^{-1} (trace b) at different pH values: 2.0 (A), 3.0 (B), 4.0 (C) and 7.0 (D). Always shown the 3rd stable scan. Inset figures show the 1st, 50th and the 100th scans from the immobilization procedure at 100 mVs^{-1}at pH 2.0, 3.0, 4.0 and 7.0.

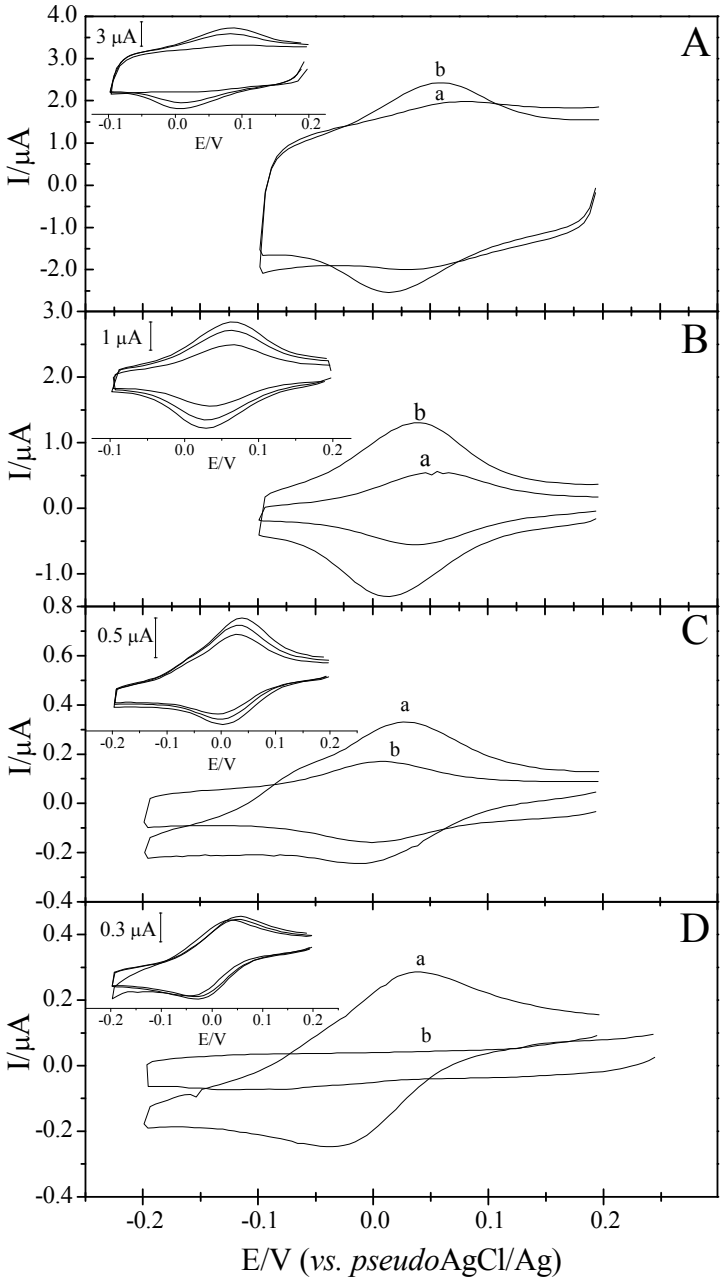

View Article Online
DOI: 10.1039/C3AN02137H

Figure 5. (A) Catalytic response for adsorbed cyt-c/SPGEs at 0.1M PBS pH 2.0 at -0.5 V (*vs. pseudo*Ag/AgCl) with increasing amounts of H_2O_2. The arrows mark the points when the H_2O_2 aliquot was added. (B) Lineweaver-Burk plot was used to yield the K_m and i_{max} parameters.

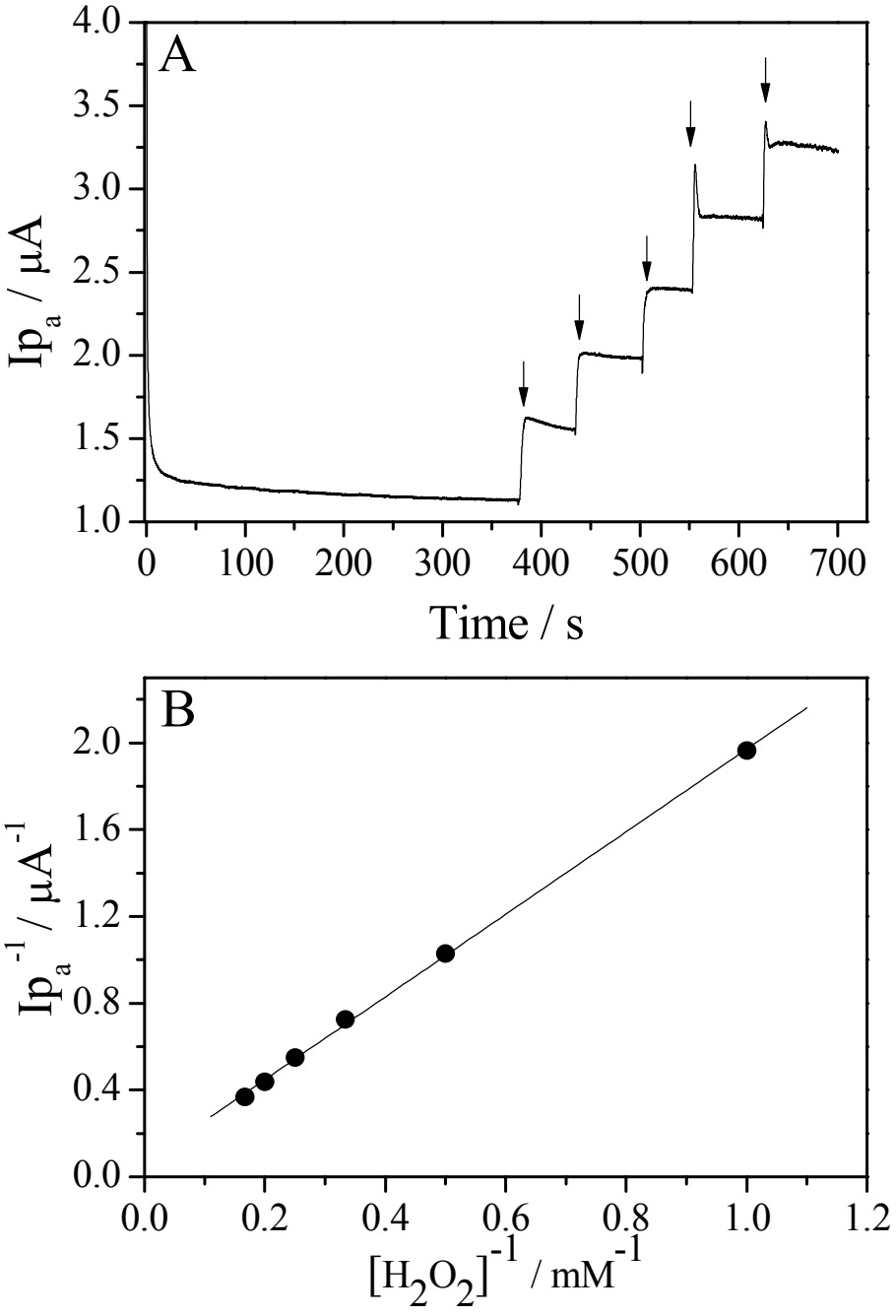

View Article Online
DOI: 10.1039/C3AN02137H

Figure 6. Steady-state current intensity response of cyt-c immobilized on the SPGE following successive injections of 1mM bulk concentration of H_2O_2 into PBS solution pH 2.0, 3.0 and 7.0.

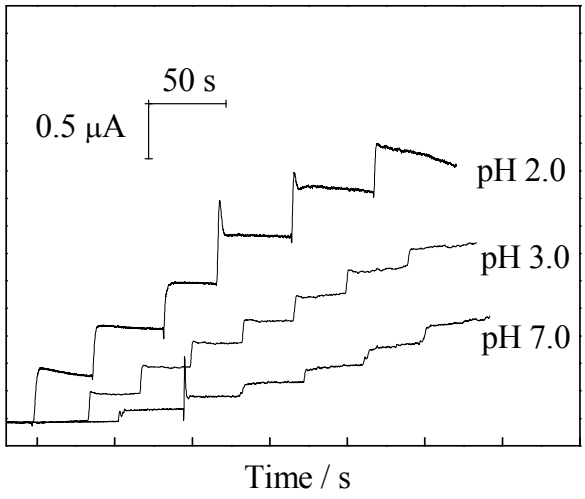

View Article Online
DOI: 10.1039/C3AN02137H

References

[1] J. Hirst, *Biochem. J.*, 2010, **425**, 327.
[2] M.W. Fariss, C.B. Chan, M. Patel, B. Van Houten, S. Orrenius, *Mol. Interventions*, 2005, **5,** 94.
[3] F.L. Rodkey, E.G. Ball, *J. Biol. Chem*., 1950, **182**, 17.
[4] R.E. Dickerson, R. Timkovick, Cytochromes c, in *The Enzymes*, ed. P. D. Boyer, Academic Press Inc., London, 3er edn., 1975, vol. 11, pp. 397.
[5] P.X. Qi, R.A. Beckman, A.J. Wand, *Biochem.,* 1996, **35**, 12275.
[6] G.R. Moore, G.W. Pettigrew, in *Cytochromes c. Evolutionary, structural, and physicochemical aspects*, Springer-Verlag, Berlin, 1990.
[7] M. Ohgushi, A. Wada, *FEBS J*., 1983, **164**, 21.
[8] Y. Goto, Y. Hagihara, D. Hamada, M. Hoshino, I. Nishii, *Biochem.*, 32 (1993) 11878.
[9] Y. Goto, S. Nishikiori, *J. Mol. Biol*., 1991, **222**, 679.
[10] H. Christensen, R.H. Pain, *Eur. Biophys. J*., 1991, **19**, 221.
[11] G. Battistuzzi, C.A. Bortolotti, M. Bellei, G. Di Rocco, J. Salewski, P. Hildebrandt, M. Sola, *Biochem*., 2012, **51**, 5967.
[12] A. Naeem, R. Hasan Khan, Int. *J. Biochem. Cell Biol.*, 2004, **36**, 2281.
[13] A.A. Moosavi-Movahedi, J. Chamani, H. Ghourchian, H. Shafiey, C.M. Sorenson, N. Sheibani, *J. Prot. Chem*., 2003, **22**, 23.
[14] F. Marken, C. A. Paddon, D. Asogan, *Electrochem. Commun.,* 2002, **4**, 62.
[15] A.K. Abass, J.P. Hart, *Electrochim. Acta,* 2001, **46**, 829.
[16] S.-F. Ding, W. Wei, G.-C. Zhao, *Electrochem. Commun*., 2007, **9**, 2202.
[17] L. Zhu, D. Sun, T. Lu, C. Cai, C. Liu, W. Xing, *Sci. China Ser. B-Chem.,* 2007, **50**, 304.
[18] C. Lei, F. Lisdat, U. Wollenberger, F.W. Scheller, *Electroanal*., 1999, **11**, 274.
[19] M. Gómez-Mingot, J. Iniesta, V. Montiel, R.O. Kadara, C.E. Banks, *Analyst,* 2011, **136**, 2146.
[20] H.A. Theorell, A. Akesson, *J. Am. Chem. Soc*., 1941, **63**, 1804.
[21] Y.P. Myer, L.H. MacDonald, B.C. Verma, A. Pande, *Biochem*., 1980, **19**, 199.
[22] Y.P. Myer, A.F. Saturno, B.C. Verma, A. Pande, *J. Biol. Chem.,* 1980, **254**, 11202.
[23] S. Monari, D. Millo, A. Ranieri, G. Di Rocco, G. van der Zwan, C. Gooijer, S. Peressini, C. Tavagnacco, P. Hildebrandt, M. Borsari, *J. Biol. Chem.,* 2010, **15**, 1233.
[24] L. Banci, I: Bertini, G. Cavallaro, C. Luchinat, *J. Biol. Chem*., 2002, **7,** 416.
[25] W. Qin, R. Sanishvili, B. Plotkin, A. Schejter, E. Margoliash, *Biochim. Biophys. Acta,* 1995, **1252**, 87.
[26] J.B. Wooten, J.S. Cohen, I. Vig, A. Schejter, *Biochem*., 1981, **20**, 5394.
[27] E. Laviron, *J. Electroanal. Chem*., 1979, **101**, 19.
[28] R. Schweitzer-Stenner, R. Shah, A. Hagarman, I. Dragomir, *J. Phys. Chem. B,* 2007, **111**, 9603.
[29] T. Pineda, J.M. Sevilla, A.J. Román, M. Blázquez, *Biochim. Biophys. Acta*, 1997, **1343**, 224.
[30] E. Laviron, *J. Electroanal. Chem*., 1979, **100,** 263.
[31] L. Zhang, *Biosens. Bioelectron*., 2008, **23**, 1610.
[32] R.E. Dickerson, T. Tanako, D. Eisenberg, O.B. Kallai, L. Samson, A. Cooper. E. Margoliash, *J. Biol. Chem*., 1971, **246**, 1511.
[33] N.H. Kim, M.S. Jeong, S.Y. Choi, J.H. Kang, *Mol. Cells,* 2006, **22**, 220.
[34] S. Raha, B.H. Robinson, *Trends Biochem. Sci*., 2000, **25**, 502.
[35] M.J. Davies, *Biochim. Biophys. Acta,* 2005, **1703**, 93.
[36] K. Habermüller, M. Mosbach, W. Schuhmann, Fresen. *J. Anal. Chem*., 2000, **366**, 560.
[37] P.K. Witting, A.G. Mauk, P.A. Lay, *Biochem*., 2002, **41**, 11495.
[38] S.Y. Qian, Y.R. Chen, L.J. Deterding, Y.C. Fann, C.F. Chignell, K.B. Tomer, R.P. Mason, *Biochem*., 2002, **363**, 281.
[39] A.K. Yagati, T.Lee, J. Min, J.-W. Choi, *Colloid. Surface. B*., 2012, **92**, 161.

View Article Online
DOI: 10.1039/C3AN02137H

[40] L. Wang, D.H. Waldeck, *J. Phys. Chem. C,* 2008, **112**, 1351.
[41] M. Gómez-Mingot, L.A. Alcaraz, J. Heptinstall, A. Donaire, M. Piccioli, V. Montiel, J. Iniesta, Arch. *Biochem. Biophys*., 2013, **529**, 26.
[42] R.A. Kamin, G.S. Wilson, *Anal. Chem*., 1980, **52**, 1198.
[43] H. Ju, S. Liu, B. Ge, F. Lisdat, F. W. Scheller, *Electroanal*., 2002, **14**, 141.